Comment on "Numerical investigation of optically induced director oscillations in nematic liquid crystals"

E. Brasselet
Laboratoire de Physique UMR 5672, École Normale Supérieure de Lyon, 46 Allée d'Italie, 69364 Lyon Cedex 07, France
(Received 9 December 2004; published 8 July 2005)

A nonlinear optical system based on nematic liquid crystals film was numerically investigated by Demeter and Kramer in [Phys. Rev. E **64**, 020701(R) (2001)]. They show that the uncommon route to chaos via a cascade of homoclinic gluing bifurcations predicted by a perturbative approach surprinsingly does not exist when the problem is solved exactly. On the other hand, the system still exhibits a secondary instability but its threshold is found to be much higher than previously reported. We clarify the reason for the failure of the perturbative approach and its limits of applicability. Moreover, the significant increase of the secondary instability threshold can be understood from a nonrealistic amplification of light intensity introduced by the perturbative model.

DOI: 10.1103/PhysRevE.72.013701 PACS number(s): 42.70.Df, 42.65.Sf, 05.45.Ac

The nonresonant optical reorientation of liquid crystals is unique in the sense that the light itself is altered by the induced modifications that may lead to several kinds of self-sustained oscillations. In the particular case of homeotropic nematic liquid crystals films (where the director $\boldsymbol{n}$ is perpendicular to the cell walls at boundaries), we can mention the following pioneering works that have reported the observation of an oscillatory behavior in different light-matter interaction geometries: an ordinary linearly polarized light at small oblique incidence [1], a circularly [2], or elliptically [3] polarized light at normal incidence, and a linearly polarized light beam having an elliptic intensity profile whose major axis is perpendicular to the polarization direction [4]. Among these situations the first one [Fig. 1(a)] has emerged as configuration which could lead to the observation of a transition to chaos [5].

An uncommon route to chaos via a cascade of homoclinic gluing bifurcations [6] was predicted when the light intensity is taken as the control parameter [7]. However, despite several attempts to observe the predicted cascade only what seems to be the first steps of the scenario (a secondary Hopf bifurcation followed by a gluing bifurcation) has been clearly identified experimentally by using standard reconstruction methods [8,9]. In addition, the experimental indication that a second gluing bifurcation could take place has been reported independently in [9,10].

More recently, Demeter and Kramer [11] carried out numerical investigations and proved that the inclusion of additional higher order spatial modes [$\phi_{n\geqslant 3}$ and $\theta_{n\geqslant 2}$ with $\phi=\Sigma\phi_n \sin(n\pi z/L)$ and $\theta=\Sigma\theta_n \sin(n\pi z/L)$, see Fig. 1(b)] together with the exact resolution of Maxwell's equations has the following consequences. The first gluing bifurcation threshold is significantly increased in comparison with the perturbative model [7]. Second, the gluing cascade scenario is surprisingly not observed in the simulations although it may exist in a finite range of parameters (angle of incidence and intensity) [11]. Finally, chaos may even not be predicted in a situation where it has been nevertheless observed experimentally [8,9,11]. However, the limits of the applicability of a perturbative approach which more generally is essential to justify the need for an exact resolution, were not discussed. In this Comment, we clarify these points which underlines a general difficulty encountered when solving the light propagation problem in an inhomogeneous and anisotropic medium, where both phase and energy exchanges between proper waves can take place.

For the purpose of demonstration, we present the quantitative comparison between the perturbative model presented in [7] with exact numerical simulations, using the same minimal set of variables $\mathbf{x}=(\phi_1,\phi_2,\theta_1)$. In both cases, the time evolution of the system can be written as $\dot{\mathbf{x}}=\mathbf{F}(\mathbf{x})$ where the dot indicates time derivative. There, the functions F_i are integrals over z involving optical quantities that have to be numerically calculated separately by solving the light propagation in the medium when the problem is treated exactly. On the other hand, these functions turn out to be explicit sums of terms $\phi_i^\alpha\theta_j^\beta$ ($\alpha+\beta\leqslant 3$ to the lowest order [7]). Contrarily to the simulations of Demeter and Kramer [11], the present calculations include the elastic anisotropy, all other assumptions being the same (infinite plane wave, slowly varying envelope approximation, no backward propagating modes, and no backflow). Consequently, the perturbative and the exact approaches will be further compared on the same basis.

The input beam intensity I_y^{in} is taken as the control parameter and we define the intensity of the electric field component along the x and y axes at the output of the film, $I_{x,y}^{\text{out}}$, as the observables. This choice is motivated by the will to deal

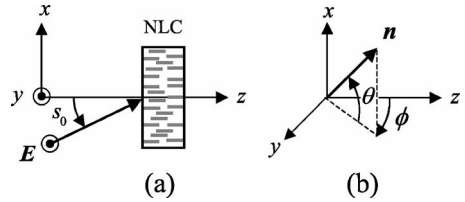

FIG. 1. (a) Interaction geometry: an ordinary light wave illuminates a homeotropically aligned nematic liquid crystal cell at oblique incidence; (b) representation of the director $\boldsymbol{n}$ with the two angles ϕ and θ.

with quantities that can be easily assessed experimentally. In fact, these observables were originally used in the earlier experimental demonstration of a chaotic dynamics [5]. We further introduce the normalized length and intensity $\xi = z/L$ and $\rho = I_y^{\text{in}}/I_F$, where I_F is the Fréedericksz transition threshold for linear polarization at normal incidence, and the normalized intensities $\tilde{I}_{x,y}(\xi,t) = I_{x,y}(\xi,t)/I_y^{\text{in}}$. As far as the perturbative model is concerned, one can show that

$$\tilde{I}_x(\xi,t) = \frac{\kappa^2\pi^2}{s^2}\left((\mathcal{L}_1[\phi])^2 - \frac{2}{s}\mathcal{L}_1[\phi]\mathcal{L}_1[\phi\theta]\right), \tag{1}$$

$$\tilde{I}_y(\xi,t) = 1 - \frac{2\kappa^2\pi^2}{s^2}\mathcal{L}_2[\phi,\phi], \tag{2}$$

where $\mathcal{L}_1[f](\xi,t) = \int_0^\xi f(\xi',t)d\xi'$ and $\mathcal{L}_2[f,g](\xi,t) = \int_0^\xi g(\xi',t)\int_0^{\xi'} f(\xi'',t)d\xi''d\xi'$. This leads to the following expressions for the observables:

$$\tilde{I}_x^{\text{out}}(t) = \frac{4\kappa^2}{s^2}\left(1 - \frac{\pi}{2s}\theta_1(t)\right)\phi_1^2(t), \tag{3}$$

$$\tilde{I}_y^{\text{out}}(t) = 1 - \frac{4\kappa^2}{s^2}\phi_1^2(t), \tag{4}$$

where $\kappa = (L/\lambda)(s_0^2\epsilon_a/\epsilon_\parallel\epsilon_\perp^{1/2})$, λ being the wavelength of light, $\epsilon_\parallel(\epsilon_\perp)$ the dielectric permittivity along (perpendicular) to $\boldsymbol{n}$, $\epsilon_a = \epsilon_\parallel - \epsilon_\perp$ and $s = s_0/\epsilon_\perp^{1/2}$ with s_0 the external angle of incidence [Fig. 1(a)]. In these expressions, ϕ_1 and θ_1 are solutions of the system of equations given in [7]. On the other hand, the quantities $\tilde{I}_{x,y}^{\text{out}} = |E_{x,y}(z=L,t)/E_y(z=0,t)|^2$ are calculated from the integration of a pair of ordinary differential equations governing the propagation of the electric field when the problem is solved exactly. The corresponding equations write $\partial\mathbf{E}_\perp/\partial z = \mathbf{G}(\mathbf{x},z)$ with the boundary condition $\mathbf{E}_{\perp,z=0} \propto (0,\sqrt{\rho})$, where $\mathbf{E}_\perp = (E_x,E_y)$ and since the detailed expression of $\mathbf{G}$ is not of major interest here, we consequently do not reproduce it hereafter. It is simply worth noting that the derivation scheme is based on Oldano formalism [12] and it could be found in [7]. The following values were used for calculations $L = 50\ \mu$m, $\lambda = 514.5$ nm, $s_0 = 7°$, $\epsilon_\perp = 2.25$, $\epsilon_\parallel = 3.01$, and the ratio of the Frank elastic constant $K_1/K_3 = 2/3$ and $K_2/K_3 = 1/2$, which are those of [7].

The intensity dependence of the pair of observables are shown in Fig. 2(a) (perturbative approach) and 2(b) (exact approach) where the minima and maxima of $\tilde{I}_x^{\text{out}}$ (solid lines) and $\tilde{I}_y^{\text{out}}$ (dashed lines) are presented. As it is already known, both situations give the same first stages for the bifurcation scenario [7,11]: (i) a primary bifurcation at $\rho = \rho_c$ leading to a time-independent distorted state, (ii) a secondary supercritical Hopf bifurcation at $\rho = \rho_0$ where the director starts to oscillate periodically, (iii) a gluing bifurcation at $\rho = \rho_1$ where two limit cycles which are mutual image under the transformation $(\phi,\theta) \to (-\phi,\theta)$ merge in a single double length limit cycle. More precisely, this transition threshold sequence (ρ_c,ρ_0,ρ_1) is found to be (1.063, 1.717, 1.809) for the perturbative approach and (1.063, 1.730, 2.035) for the exact approach. The significant increase of ρ_1, when the problem is solved exactly instead of perturbatively, was mentioned in [11] and we would like to point out that an accurate quantitative experimental validation can be found in [10]. In addition, we found that a straightforward perturbative expansion of *all* the functions involved in the problem (incuding the light field) up to the third order for the angles (θ,ϕ) turns out to be invalid although the necessary condition $\theta^2, \phi^2 \ll 1$ remains satisfied. Indeed, one should expect the physical constraint $0 \leqslant \tilde{I}_{x,y}^{\text{out}} \leqslant 1$ to be satisfied, at least within an acceptable margin of error:

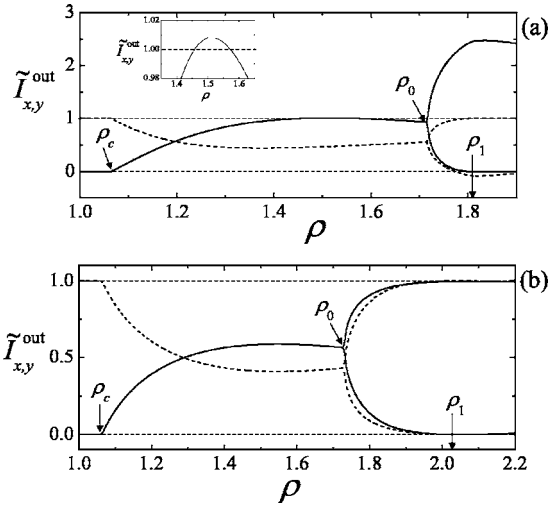

FIG. 2. Extrema of $\tilde{I}_x^{\text{out}}$ (solid lines) and $\tilde{I}_y^{\text{out}}$ (dashed lines) vs the normalized intensity ρ; (a) perturbative model where the inset presents an enlargement around $\rho = 1.5$; (b) exact model.

$$-\delta I \leqslant \tilde{I}_{x,y}^{\text{out}} \leqslant 1 + \delta I \quad \text{with} \quad \delta I \ll 1. \tag{5}$$

From Fig. 2, this constraint is satisfied below the Hopf bifurcation where $\delta I < 0.01$ (see the inset). However, above the Hopf bifurcation $\delta I \sim 1$ and the perturbative approach fails. More precisely, Fig. 3 illustrates how the previous constraint is violated in the bulk of the liquid crystal at $\rho = 1.01\rho_1$, where a cumulative effect during the light propagation is clearly seen. We therefore have to conclude that the route to chaos via a gluing bifurcation cascade cannot be retained from the very begining. In addition, the present findings shed light on the surprising shift to the region of higher intensities of the bifurcation line that corresponds to $\rho = \rho_1$ in the plane of parameters (ρ, s_0) when the light propagation problem is solved exactly, that was reported in [11]. Qualitatively, this could be understood from the fact that the optical torque is obviously higher than it should be in the perturbative model which introduces a nonrealistic light amplification [see Fig. 3(a)].

Incidentally, the director trajectory in the (ϕ_1,ϕ_2,θ_1) phase space remains qualitatively the same in both approaches. This is illustrated in Fig. 4 where the trajectories are presented between the Hopf and the gluing bifurcation, at $\rho = (\rho_0+\rho_1)/2$ (gray lines), and slightly above the gluing bifurcation, at $\rho = 1.01\rho_1$ (black lines), for both approaches. It allows us to understand why the gluing cascade scenario,

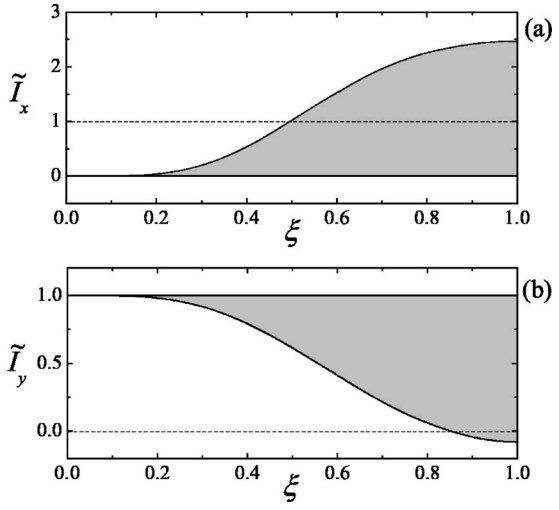

FIG. 3. Gray regions represent the range of values explored in time by $\tilde{I}_x(\xi,t)$ (a) and $\tilde{I}_y(\xi,t)$ (b) vs the normalized length ξ in the perturbative model at $\rho=1.01\rho_1$, which corresponds to the limit cycle behavior plotted in black in Fig. 4(a).

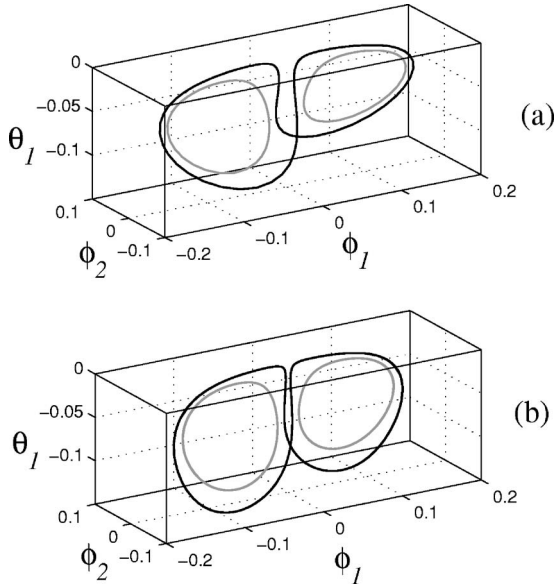

FIG. 4. Director trajectories at $\rho=(\rho_0+\rho_1)/2$ (gray) and $\rho=1.01\rho_1$ (black); (a) perturbative model; (b) exact model.

despite revealed in the present work to be an artifact of the perturbative model, could not have been invalidated by observations [9].

In summary, although it is enough to retain a minimal number of reorientation spatial modes to catch the principal dynamical features of the present optical system, it is necessary to solve exactly the light propagation problem [13]. Actually, the limit of the applicability of the perturbative approach is restricted to an intensity not higher than the secondary instability threshold. At higher intensities, an exact treatment becomes compulsory. The quantitative description of all the reported experimental observations is nevertheless still far from being completed. The present results thus invite one to pay particular attention to the light propagation problem when deriving further improved models. For instance, we can mention that the inclusion of transverse nonlocal effects arising from the finite size of the excitation beam, at least from a perturbative manner, must be carried out by solving the light propagation problem exactly.

The author is grateful to G. Demeter, L. Kramer, M. Fauquembergue, and L. J. Dubé for discussions.

[1] A. S. Zolot'ko, V. F. Kitaeva, N. Kroo, N. N. Sobolev, and L. Csillag, Pis'ma Zh. Eksp. Teor. Fiz. **32**, 170 (1980); [JETP Lett. **32**, 158 (1980)].
[2] E. Santamato, B. Daino, M. Romagnoli, M. Settembre, and Y. R. Shen, Phys. Rev. Lett. **57**, 2423 (1986); A. S. Zolot'ko, V. F. Kitaeva, and V. Y. Fedorovich, Preprint 326, P. N. Lebedev Physics Institute, Academy of Sciences of the USSR, Moscow, 1986.
[3] E. Santamato, G. Abbate, P. Maddalena, L. Marrucci, and Y. R. Shen, Phys. Rev. Lett. **64**, 1377 (1990).
[4] B. Piccirillo, C. Toscano, F. Vetrano, and E. Santamato, Phys. Rev. Lett. **86**, 2285 (2001).
[5] G. Cipparrone, V. Carbone, C. Versace, C. Umeton, R. Bartolino, and F. Simoni, Phys. Rev. E **47**, 3741 (1993).
[6] A. Arneodo, P. Coullet, and C. Tresser, Phys. Lett. **81**, 197 (1981); Y. Kuramoto and S. Koga, Phys. Lett. **92**, 1 (1982).
[7] G. Demeter and L. Kramer, Phys. Rev. Lett. **83**, 4744 (1999); G. Demeter, Phys. Rev. E **61**, 6678 (2000).
[8] G. Russo, V. Carbone, and G. Cipparrone, Phys. Rev. E **62**, 5036 (2000).
[9] V. Carbone, G. Cipparrone, and G. Russo, Phys. Rev. E **63**, 051701 (2001).
[10] E. Santamato, P. Maddalena, L. Marrucci, and B. Piccirillo, Liq. Cryst. **25**, 357 (1998).
[11] G. Demeter and L. Kramer, Phys. Rev. E **64**, 020701(R) (2001).
[12] C. Oldano, Phys. Rev. A **40**, 6014 (1989).
[13] In fact, this has been revealed to be fruitful in another interaction geometry where the excitation beam is circularly polarized at normal incidence. In that case, a secondary instability missed in earlier investigations thus could be predicted [E. Brasselet, B. Doyon, T. V. Galstian, and L. J. Dubé, Phys. Lett. A **299**, 212 (2002)].